JBC RESEARCH ARTICLE

Serine 970 of RNA helicase MOV10 is phosphorylated and controls unfolding activity and fate of mRNAs targeted for AGO2-mediated silencing

Received for publication, September 26, 2022, and in revised form, February 24, 2023 Published, Papers in Press, March 5, 2023,
https://doi.org/10.1016/j.jbc.2023.104577

Aatiqa Nawaz[1], Phillip J. Kenny[1], Temirlan Shilikbay[1], Matt Reed[2], Olga Stuchlik[2], Jan Pohl[2], and Stephanie Ceman[1,*]

From the [1]Department of Cell and Developmental Biology, University of Illinois-Urbana Champaign, Champaign, Illinois, USA; [2]Biotechnology Core Facility Branch, Centers for Disease Control and Prevention, Atlanta, Georgia, USA

Reviewed by members of the JBC Editorial Board. Edited by Karin Musier-Forsyth

MOV10 is an RNA helicase required for organismal development and is highly expressed in postnatal brain. MOV10 is an AGO2-associated protein that is also necessary for AGO2-mediated silencing. AGO2 is the primary effector of the miRNA pathway. MOV10 has been shown to be ubiquitinated, leading to its degradation and release from bound mRNAs, but no other posttranslational modifications with functional implications have been described. Using mass spectrometry, we show that MOV10 is phosphorylated in cells at the C-terminus, specifically at serine 970 (S970). Substitution of S970 to phospho-mimic aspartic acid (S970D) blocked unfolding of an RNA G-quadruplex, similar to when the helicase domain was mutated (K531A). In contrast, the alanine substitution (S970A) of MOV10 unfolded the model RNA G-quadruplex. To examine its role in cells, our RNA-seq analysis showed that the expression of S970D causes decreased expression of MOV10 enhanced Cross-Linking Immunoprecipitation targets compared to WT. Introduction of S970A had an intermediate effect, suggesting that S970 was protective of mRNAs. In whole-cell extracts, MOV10 and its substitutions bound AGO2 comparably; however, knockdown of AGO2 abrogated the S970D-induced mRNA degradation. Thus, MOV10 activity protects mRNA from AGO2; phosphorylation of S970 restricts this activity resulting in AGO2-mediated mRNA degradation. S970 is positioned C-terminal to the defined MOV10–AGO2 interaction site and is proximal to a disordered region that likely modulates AGO2 interaction with target mRNAs upon phosphorylation. In summary, we provide evidence whereby MOV10 phosphorylation facilitates AGO2 association with the 3′UTR of translating mRNAs that leads to their degradation.

miRNAs regulate approximately half of the expressed genes (1). The essential effector proteins of the miRNA pathway like Argonaute 2 (AGO2) are known, but how the miRNA recognition element (MRE) in the 3′UTR is modulated by RNA-binding proteins (RBPs) for AGO2 association is still unknown. MOV10 is an RNA helicase that is an important cofactor for AGO1- and AGO2-mediated translational suppression (2). MOV10 moves in a 5′ to 3′ direction on an RNA through its helicase domain in an ATP-dependent manner (3). MOV10 can either facilitate AGO2 association with its MREs or block its association with MREs, depending on the secondary structure of the RNA and associated RBPs (4). 3′ UTRs contain the most G-quadruplex structures (rG4s) among the gene regions surveyed (5). Thus, rG4s likely play an important regulatory role in the 3′UTR. MOV10 preferentially binds G-rich regions in mRNAs, including rG4s (4). In addition to associating with them, MOV10 is also able to unfold rG4s (6), which we demonstrated using iSpinach, an RNA aptamer that contains an rG4 structure that is necessary to bind the 3,5-difluoro-4-hydroxybenzylidene imidazolinone fluorophore. Upon binding 3,5-difluoro-4-hydroxybenzylidene imidazolinone, the complex fluoresces as a green fluorescent mimic so unfolding of the rG4 can be measured as a loss of fluorescence (7–9). We found that MOV10 is able to unfold the iSpinach aptamer in an ATP-dependent manner (6).

MOV10, as well as many of its associated RBPs, including FMRP, are regulated by posttranslational modifications (4, 6). MOV10 is one of the most enriched RBPs in neurites, suggesting an important role in these structures. In neurons, N-methyl-D-aspartate stimulation results in the ubiquitination of MOV10 and its consequent degradation, which releases a subset of mRNAs for translation (10, 11). Here, we identified a phosphorylation site of MOV10 and the consequence of that modification on cellular function.

Results

We began this study by examining the mobility shift of lambda phosphatase treated or nontreated myc-MOV10 immunoprecipitated from the murine neuroblastoma cell line Neuro 2a (N2A) in a gel containing Phos-tag reagent. Phos-tag reagent captures phosphate groups, leading to a mobility shift of phosphorylated modified proteins on a resolving gel (12). We observed a slower band in the myc-MOV10 IP that was eliminated upon phosphatase treatment,

* For correspondence: Stephanie Ceman, sceman@illinois.edu.

suggesting that MOV10 was indeed phosphorylated in N2A (Fig. 1*A*).

MOV10 has an N-terminal domain that functions primarily as a protein interaction domain required for neurite outgrowth (6) and blocking HIV infection (13). In contrast, the C-terminal domain contains the recA domains, which confer its helicase properties. To determine on which domain phosphorylation occurred, extracts of N2A cells expressing either the N-terminal or C-terminal domains of MOV10 were resolved on a Phos-tag gel. Only the C-terminal domain showed a doublet in contrast to the N-terminal domain, suggesting that phosphorylation occurred there (Fig. 1*B*).

To obtain microgram quantities of MOV10, Myc-MOV10 was isolated after transfection of HEK293F cells (Fig. S1), digested with trypsin and run on a Lumos nanoHPLC-MSMS system. Using three different search algorithms, an identical site, serine 970 in murine MOV10 was identified as phosphorylated (Fig. 1*C*). Similarly, in a large-scale screen for cell cycle–dependent phospho-events, this residue was one of the seven MOV10 phosphosites identified in a global phosphoproteome study that quantified 6027 proteins and 20,443 unique phosphorylation sites (14).

To identify a function for this phosphosite, an alanine was introduced at position 970 to render MOV10 constitutively unphosphorylated (S970A), while the negatively charged aspartic acid was introduced at position 970 to mimic constitutive phosphorylation (S970D). Because the phosphosite was proximal to the helicase domain and because we had previously shown that MOV10 was able to unfold the model rG4, iSpinach (6), we examined the activity of purified MOV10 mutants S970A and S970D along with the helicase mutant K531A (Fig. S2) in this assay. Introduction of an alanine had no effect on MOV10's ability to unfold an rG4. In contrast, S970D, like the helicase mutant, was unable to unfold the iSpinach aptamer, suggesting that phosphorylation blocks the unfolding activity of MOV10 (Fig. 2*A*).

Using another model rG4, Sc1, which we have shown binds MOV10 (4), we confirmed that the C-terminus of MOV10 bound Sc1 more efficiently than its mutated structure (Sc1mut) (Fig. 2*B*). To demonstrate that the impaired unfolding by S970D was not due to an inability to bind rG4s, we performed Sc1 capture experiments of the purified proteins and determined that mutation of S970 had no effect on the ability of either protein to bind RNA rG4s (Fig. 2*C*). To examine whether serine 970 is located in or near a predicted RNA-binding site, we evaluated MOV10's C-terminus for the characteristic sequence motifs shared by SF1 helicases (15) (Fig. 2*D*). In the primary sequence of the C-terminus of MOV10, S970 is distal to the predicted RNA-binding motifs, boxed in blue. Thus, S970 is not in a predicted nucleic acid–binding site.

To examine the effect of position 970 of MOV10 on steady-state levels of RNA, we transfected a MOV10 KO N2A line described in (15) with either WT MOV10 or S970D or S970A, isolated total RNA and identified 15,977 genes of which 6419 genes were significantly changed among the three conditions, which was performed three times (Fig. 3*A*). A representative Western blot shows equal transgene expression (Fig. 3*B*), which was confirmed in the RNA-seq. The WT and S970D treatments were distinctly different from each other, with S970A intermediate in changed RNAs but closer to WT (Fig. 3*A*). Because the S970D *versus* WT pairwise comparison had so many more genes changed (6939) than S970A *versus* WT (2010), we adjusted for multiple testing correction by doing a "global" False Discovery Rate correction across *p*-values for all three comparisons together (Supporting Information Data 1 and Table S1). This ensured that a gene with the same raw *p*-value in two different comparisons would not end up with vastly different FDR *p*-values.

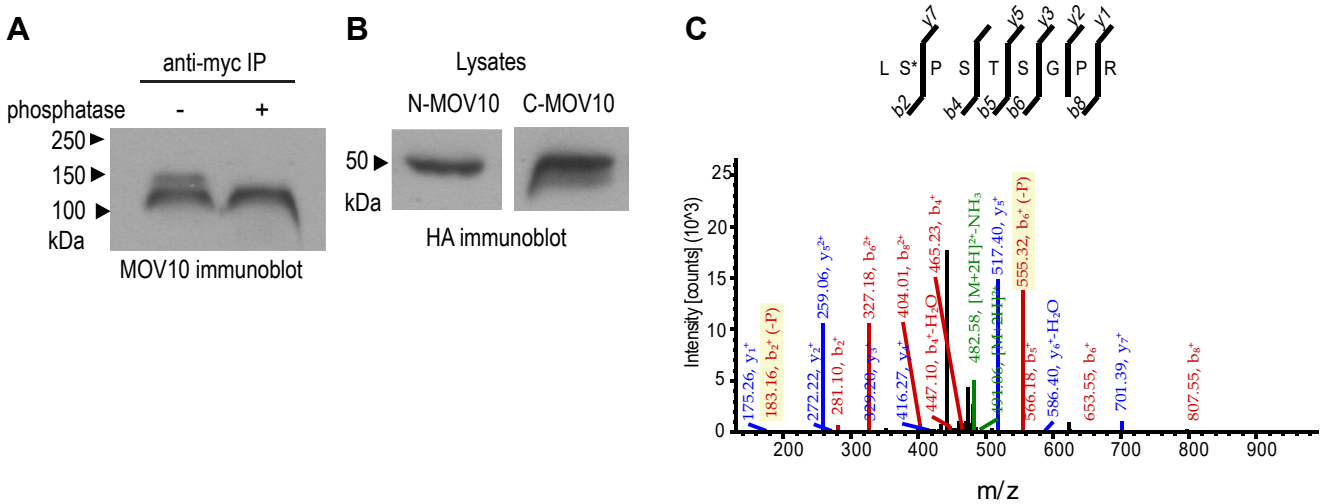

Figure 1. Murine MOV10 is phosphorylated on serine 970. *A*, immunoprecipitated myc-murine MOV10 was untreated (–) or treated (+) with phosphatase and resolved in a 7.5% Phos-tag SDS-PAGE gel and immunoblotted with an antibody to MOV10. *B*, lysates from N2A cells transfected with the HA-tagged N-terminus of MOV10 or the C-terminus of MOV10 were resolved in a 10% phos-tag SDS-PAGE gel and immunoblotted with antibody to HA. *C*, peptide sequence showing phosphorylation at S970 in myc-MOV10 identified in LC/MS/MS. *indicates phosphorylated serine. N2A, neuro 2a; S970, serine 970.

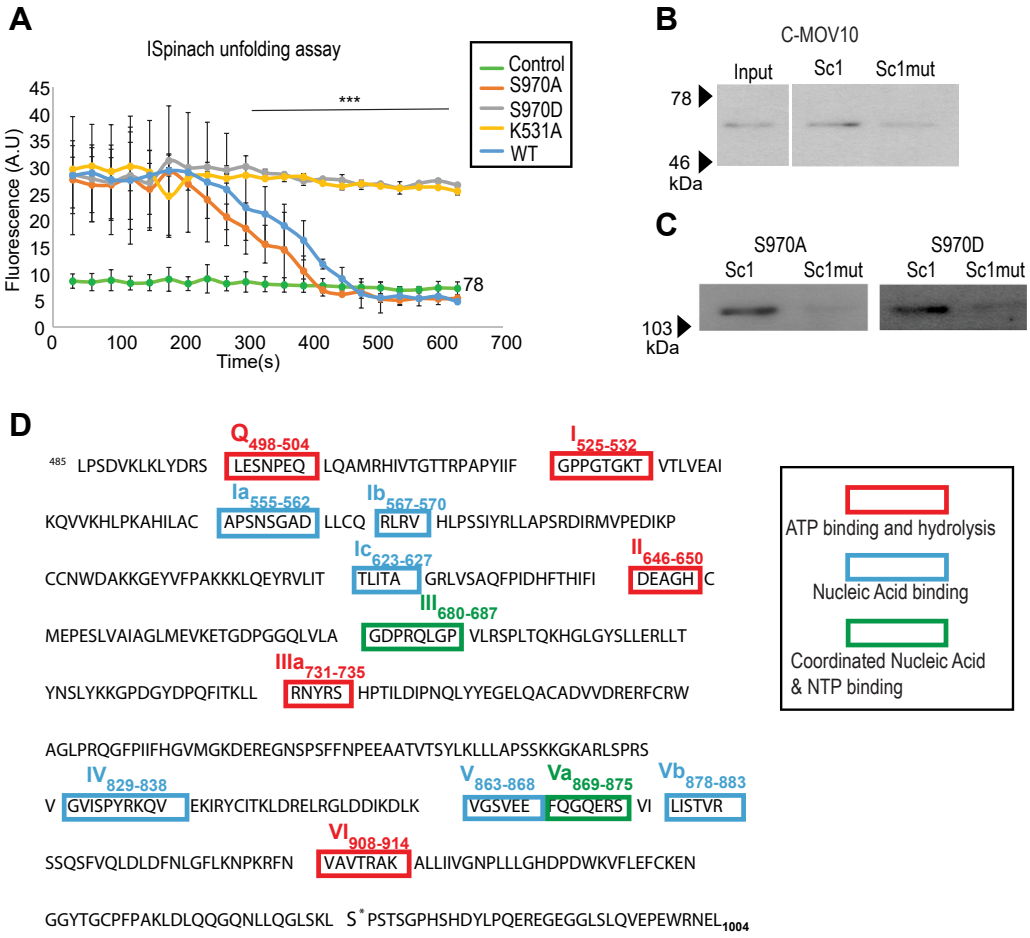

Figure 2. Amino acid at position 970 of MOV10 controls rG4 unfolding but not binding. *A*, purified murine MOV10 WT (*blue*) or with substitutions S970A (*orange*), S970D (*gray*), K531D (*yellow*) was incubated with a synthesized rG4 reporter (iSpinach) and DFHB1; ATP was added and fluorescence was recorded every 30 s using a SpectraMax M2 microplate reader (ex: 492 nm/em: 516 nm). The control (*green*) is MOV10 protein with ATP in the absence of DFHB1. The experiment was performed three times, error bars represent S. D, ***$p < 0.0001$, Two-way ANOVA followed by pairwise *t* test with Bonferroni correction for multiple testing. *B* and *C*, model rG4 (Sc1) and Sc1-mutant (Sc1 mut) capture assays using purified recombinant C-term of MOV10 and 970 substitutions. *D*, C-terminus with motifs identified in Fairman-Williams *et al.* (31). The sequence aligns with GenBank: CAA36803.1. DFHB1, 3,5-difluoro-4-hydroxybenzylidene imidazolinone; rG4s, G-quadruplex structure; S970, serine 970.

To examine the fate of the directly bound mRNAs, we first performed enhanced Cross-Linking Immunoprecipitation (eCLIP) on the replicates of MOV10 isolated from N2A cells (Figs. S3 and S4). Clusters were identified within the IP samples that contained multiple over-lapping reads. Each peak was normalized against the paired input sample. Only peaks that met a cutoff of log2 fold change ≥3 and −log10 (*p*-value) ≥3 were considered further. As expected, a large majority of significant peaks were on 3′ UTRs in both replicates. We identified 1818 high confidence MOV10-interacting RNAs (Supporting Information Data 2), which were used to make two-way Venn diagrams with the significantly changed mRNAs identified in Figure 3*A*. Importantly, downregulated genes in S970A- and S970D-expressing cells have significantly more genes with eCLIP sites than expected due to chance (Fig. 3, *E* and *F*, *p* values 9.9e-25 and 9.5e-159, respectively), while the upregulated S970A genes and S970D genes have fewer genes with eCLIP sites (Fig. 3, *C* and *D*, *p* values = 1). Thus, having an eCLIP-binding site is a strong predictor of whether an mRNA would be downregulated by S970A or S970D expression. The average fold change in downregulated genes in S970D was −1.89. In contrast, the average fold change in S970A was −1.15, suggesting that S970D has a more potent effect than S970A on a larger number of eCLIP targets. Accordingly, all of the significantly decreased S970A targets were contained within the 909 S970D targets (Fig. 3*G*). This suggests that the alanine substitution has an intermediate effect on the transcripts, underscoring the importance of a serine with its hydroxyl group having a protective effect on directly bound targets while phosphorylation mitigates that effect. The upregulation of mRNAs shown in Figure 3, *C* and *D* is likely the downstream effect of reducing eCLIP targets that had suppressive effects on transcription or transcript stability. We have shown before that MOV10 binds and regulates transcription factors (4). Presumably, they were suppressive, such that reducing their expression leads to increased expression of downstream mRNAs.

To further analyze the downregulated targets, we did a comparison with published AGO2 CLIP data (16) and found that 93% of the MOV10-bound genes downregulated in S970D

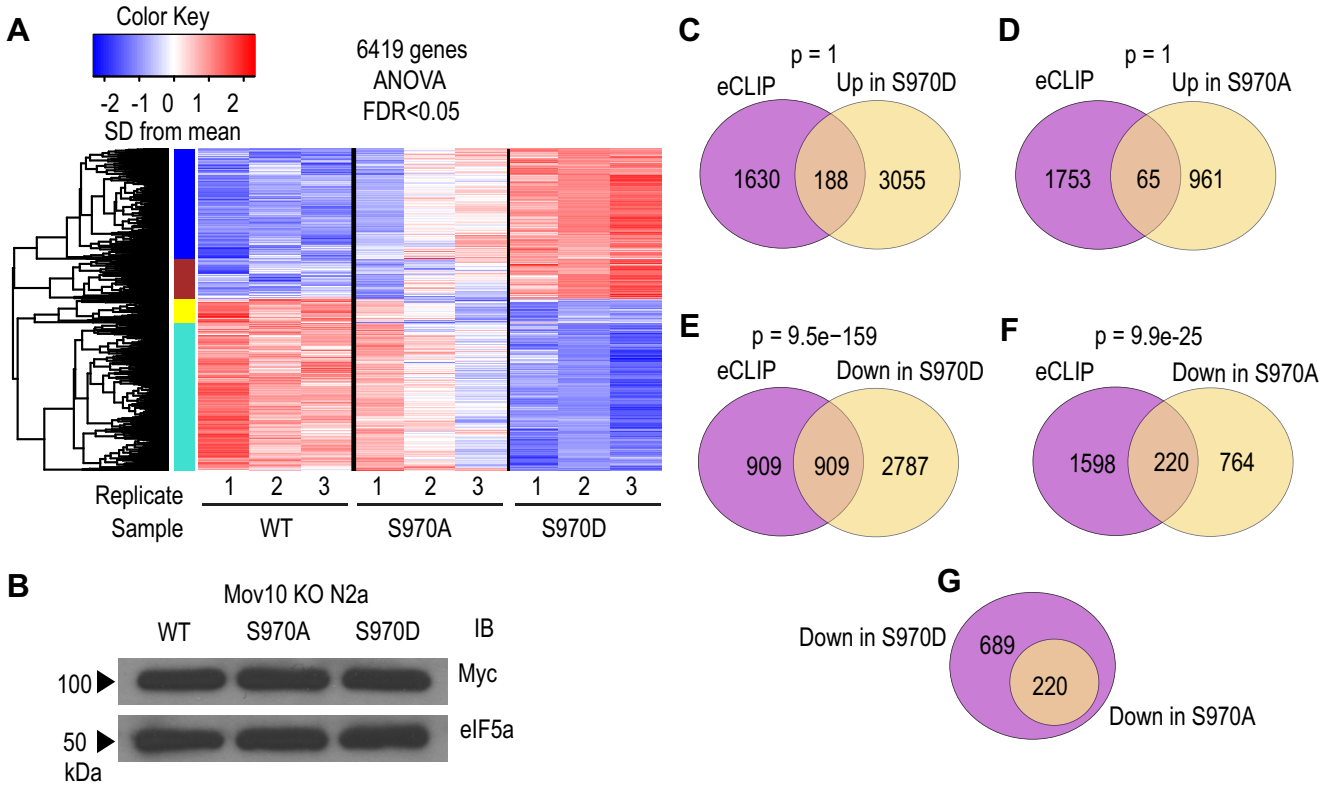

Figure 3. Substitution of S970 leads to degradation of MOV10 eCLIP mRNAs. *A*, differential gene expression analysis was performed on N2A KO transfected with MOV10 WT, S970A, or S970D and a one-way ANOVA test calculated along with all three pairwise comparisons between the three groups to identify 6419 genes visualized on a heatmap. *B*, representative Immunoblot of transfected cells probed with myc antibody for use in RNA-seq. *C–F*, Venn diagrams of MOV10 N2A eCLIP targets (*purple*) and significantly changed RNAs (*yellow*) (direction indicated) in S970A and S970D. Bootstrapping analysis showed a highly significant overlap between MOV10-bound targets that are downregulated, *p*-values are mentioned. *G*, all of the significantly reduced S970A eCLIP genes were contained within the S970D genes. eCLIP, enhanced Cross-Linking Immunoprecipitation; N2A, neuro 2a; S970, serine 970.

are shared with AGO2 targets. These targets were also represented in the mouse brain AGO2 eCLIP previously done by our lab (6). The region of MOV10 that is bound by AGO2 was identified as MOV10 residues 921 to 965, which is just upstream of S970 (17). To determine if S970D associated with more AGO2, we performed coimmunoprecipitation of MOV10 S970 mutants and WT but found no difference in binding of AGO2 with WT or the serine mutants of MOV10 or with the helicase mutant K531A (Fig. 4, *A* and *B*). Thus, there is no obvious change in AGO2 association when we look en masse at cellular extracts. We also determined the binding of WT and S970D with UPF1 and DDX6, which are known interactors of MOV10 and found no difference (Fig. S5).

To verify the RNA-seq experiment, we undertook an orthogonal approach by expressing WT, S970A, and S970D in N2A KO cells and extracting RNAs for quantitative PCR. We also compared the transgene expression to that of WT N2A and found 3 to 4 fold more expression of the transgenes (Fig. 4*C*). We compared the expression of eight MOV10 eCLIP targets in the presence of WT and S970D (Fig. 4*D*). As observed in the RNA-seq experiment in Figure 3, there was a significant reduction in the expression of the MOV10 eCLIP targets in cells expressing S970D compared to WT. We next asked whether there was a functional association with AGO2 by knocking down AGO2 (Figs. 4*E* and S6) and examining expression of the same subset of MOV10 eCLIP targets evaluated in panel D in the presence of MOV10 S970D. All the targets showed a significant increase in expression after AGO2 knockdown, suggesting that MOV10 S970D and AGO2 cooperate to downregulate these targets (Fig. 4*F*). We next asked whether MOV10 affects the intracellular localization of AGO2, specifically in puncta. MOV10 and AGO2 both associate with P-bodies and P-body marker DDX6 (18, 19). We coimmunostained MOV10 and AGO2 after transfection of N2A KO cells with WT and S970D MOV10 but observed no significant difference in the number of quantified AGO2 particles in the presence of WT or S970D MOV10. We also observed no difference in the number of DDX6 particles, however, there was a decrease in DDX6 particles in MOV10 KO cells, but the difference was not significant from WT-transfected N2A cells (Figs. S7 and S8). We conclude that residue 970 in MOV10 has a functional association with AGO2 that likely occurs in specialized areas in the cell and/or under specific conditions in the cell, like translation. As translation does not occur in P-bodies and may be required for AGO2 association and function, we suspect that S970D interaction with AGO2 may occur throughout the cytoplasm.

Using Alphafold2, we hoped to gain insight into the relationship between the AGO2-binding site (921–956), residue S970, and the remainder of the C-terminus, ending at residue 1004 (20). MOV10 has a helicase domain in its C-terminal half, and the per-residue confidence score (pLDDT) of this domain

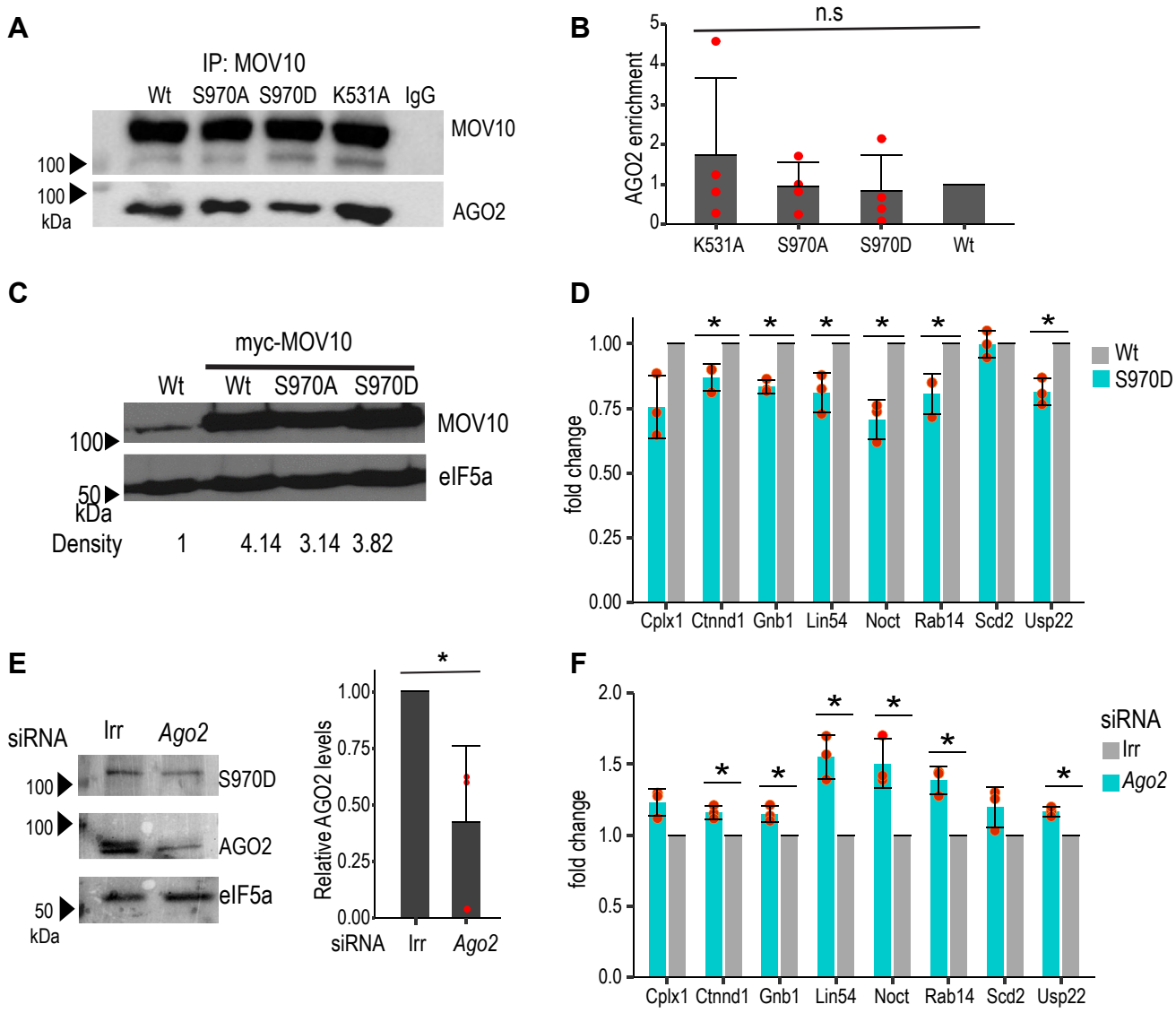

Figure 4. Reduction of S970 target mRNAs is AGO2 dependent. *A* and *B*, CO-IP of AGO2 in N2A KO cells transfected with MOV10 WT, S970A, S970D, and K531A shown in *A* and quantification shown in *B*, the experiment was repeated at least four times. *C*, Western blot of endogenous MOV10 in WT N2A cells and myc-MOV10 WT, S970A, S970D-transfected N2A KO cells. RNA isolated from WT and S970D-transfected cell samples was used to perform qPCR with select genes (*D*). *E*, Western blot of AGO2 after siRNA-mediated knockdown. Irr represents Irrelevant siRNA. N2A KO cells were cotransfected with S970D and siRNA against AGO2 and the protein levels were normalized using eIF5a. Three biological replicates were performed, the error bar represents S.D. *F*, RT-qPCR of MOV10-bound targets in the presence of S970D after AGO2 is knocked down. Error bars represent S.D., Statistical analysis was done using Student *t* test, $^{*}p < 0.05$. AGO2, Argonaute 2; Co-IP, coimmunoprecipitation; N2A, neuro 2a; S970, serine 970.

is very high (>90) and the predicted aligned error is very low (0–5 Angstroms) indicating confidence in their spatial positioning. The mapped AGO2-binding site (17) spans two amphipathic helices (turquoise) and (gray) that are unique to MOV10 by BlastP. The latter of the two helices ends with S970 followed by a region of very low pLDDT (970–1004), which could mean that either Alphafold cannot predict the structure of this region or that it is an intrinsically disordered region as predicted by MobiDB (21). Intrinsically disordered regions can modulate the binding of proteins and other molecules due to their flexibility (22), and phosphorylation of S970 could control that function (Fig. 5, *A*–*C*). In summary, we propose that the messenger ribonucleoprotein complex of MOV10 and FMRP bind the translation elongation complex, as we have shown before (4). Upon reaching the stop codon, the ribosome dissociates, and MOV10 unfolds the rG4s in the 3′UTR in a 5′ to 3′ direction (3, 6). When MOV10 becomes phosphorylated, the helicase activity stops, allowing AGO2 to recognize and bind MREs, leading to mRNA degradation (Fig. 5*D*).

Discussion

Translation of mRNAs must be tightly regulated—both temporally and spatially—likely by their association with RBPs. Outgrowth of neuronal processes is mediated by the assembly of available proteins and by new protein synthesis. As phosphorylation is an important posttranslational modification in regulating RBP function, we were interested in determining

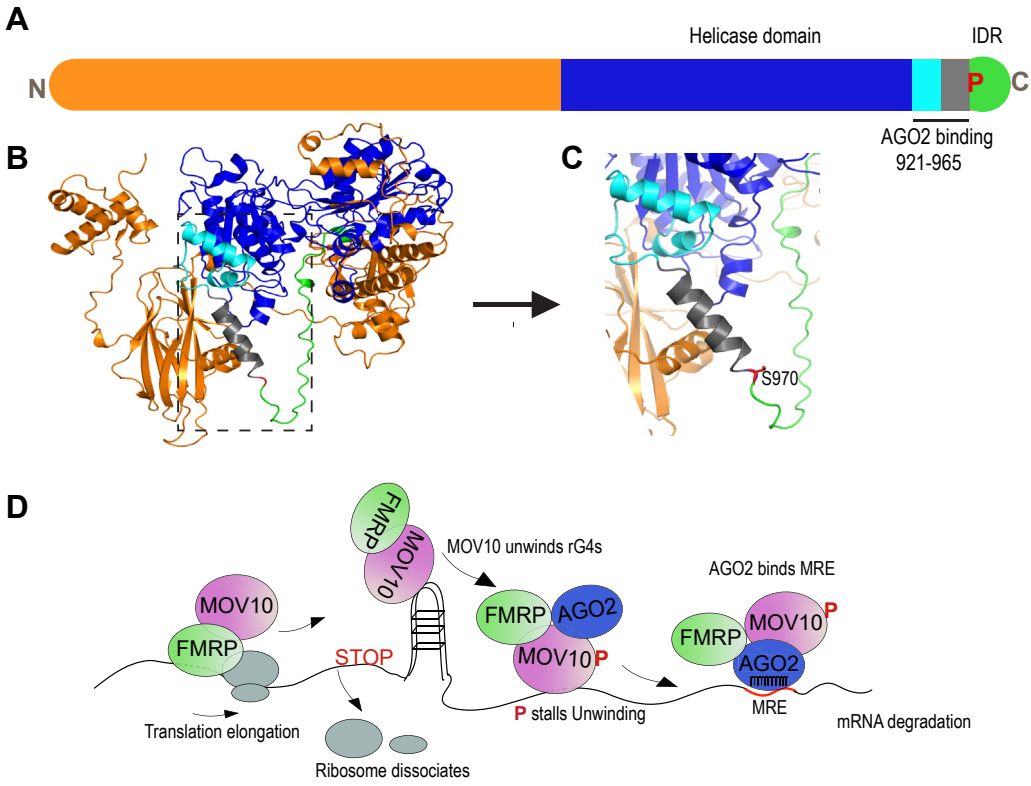

Figure 5. Phosphorylation modulates MOV10 structure and function. *A*, schematic of MOV10 primary sequence described previously (32), N-term (*orange*), helicase domain (*blue*), amphipathic helices (921–956, *turquoise*), and (956–965, *gray*), S970 is represented by P and IDR (*green*). *B*, Alphafold2 (20) structure of MOV10 with secondary structures colored as in (*A*), visualized using the PyMOL Molecular Graphics System, Version 2.0. *C*, the zoomed-in insert shows AGO2-binding sites mapped at (921–965) consisting of two amphipathic helices (*turquoise* and *gray*) followed by S970 (*red*). *D*, model for the function of phosphorylation in mRNA regulation. MOV10 is a part of the translation elongation complex along with FMRP (4, 23). At the stop codon, the ribosome dissociates and the MOV10 complex, which includes FMRP and AGO2, translocates on the RNA in 5′ to 3′ direction to unfold rG4s (3, 4). Upon phosphorylation, the unfolding stops and allows AGO2 to bind the MREs and degrade mRNAs in an miRNA-mediated manner. AGO2, Argonaute 2; IDR, intrinsically disordered region; MRE, miRNA recognition element; rG4s, G-quadruplex structure; S970, serine 970.

whether MOV10 was phosphorylated and how that affected its function.

MOV10 is both an activator and a suppressor of translation, likely through its ability to regulate AGO2 association with mRNAs (4). Our data show that changing the serine at position 970 leads to increased functional association with AGO2—particularly, when the phospho-mimic aspartic acid is introduced. This leads us to hypothesize that the serine at position 970 leads to a C-terminal conformation that precludes AGO2 association, permitting translation of bound mRNA. FMRP, a MOV10 interactor (4, 6), directly associates with ribosomes (23, 24) and AGO2 (6, 25) and may be the principal assembler of this complex, which is poised to be deposited on the 3′UTR of newly translated mRNAs. Alternatively, MOV10 may facilitate translation of its bound mRNAs indirectly. In fact, MOV10 interactor, UBAP2L (3) was recently shown to bind ribosomes directly and activate translation (26). We have also shown that MOV10 association with FMRP on rG4s blocks AGO2 association to allow translation of reporters (4, 6). About the kinase that may phosphorylate MOV10, in silico, S970 is predicted to be phosphorylated by MAPKs, including p38 kinase (NetPhos3.1 and Phosphonet). p38 was identified as regulating neurite outgrowth in rat embryonic hippocampal cultures (27). CDK5 was also identified as a possible kinase for MOV10. It will be important to identify the signal that activates the kinase cascade that phosphorylates MOV10.

Experimental procedures

Creation of mutant constructs

The murine myc-MOV10 construct was described in (4). The serine at position 970 was changed to alanine or aspartic acid using the Quick Change II Site directed mutagenesis kit (Cat #200513, Agilent) per manufacturer's instructions. PAGE-purified primers introducing the substitutions were obtained from Integrated DNA Technologies. The N- and C-terminal MOV10 plasmids were provided by (28).

Transfections, immunoprecipitations, and phosphatase treatments

N2A cells were transfected with myc-MOV10 or HA-tagged N-terminal MOV10 or HA-tagged C-terminal MOV10 as described (4). 25 μl/sample c-MYC antibody coupled agarose (A7479, Sigma-Aldrich) was used to IP MOV10 from transfected N2A cells. Lamda protein phosphatase (P0753S, NEB) was used to treat the immunoprecipitated MOV10 or lysates prepared in the absence of EDTA. Samples were mixed with 10× $MnCl_2$ and 10× reaction buffer provided with the lambda

protein phosphatase and incubated at 30 °C for 45 min. 7.5% SDS-PAGE gels were supplemented with Phos-tag AAL solution (304-93521 [AAL-107] Wako-Chemical) according to manufacturer's instructions. Large scale purifications of myc-MOV10 were from 250 to 500 ml of Freestyle HEK293F cells (Invitrogen) transfected using PEI (Cat # 408727, Sigma-Aldrich) as described (4).

MOV10 coimmunoprecipitation

MOV10 coimmunoprecipitation was performed using as described (6).

Antibodies and Western blot

Western blotting was performed as described (4, 6). The following antibodies were used: anti-MOV10 (A301-571A; Bethyl Laboratories) at 1:1000, anti-eIF5 (sc-282, Santa Cruz Biotechnology), anti-AGO2 (ab57113, Abcam), anti-DDX6 (SAB4200837, Sigma-Aldrich), anti-UPF1 (ab86057, Abcam). Secondary antibodies used were horseradish peroxidase–conjugated goat anti-rabbit (Cat # 111-035-008, Jackson Immunoresearch) and goat anti-mouse (Cat # 115-035-174, Jackson Immunoresearch). Densitometric quantification of Western blot bands was performed using imageJ following NIH protocol: https://imagej.nih.gov/ij/docs/menus/analyze.htmlCat #gels

N2A transfection and preparation for RNA-seq

2×10^5 N2A MOV10 KO [15] were plated in triplicate and transfected with plasmids bearing full-length mouse MOV10 or MOV10 S970A or MOV10 S970D. Total RNA was isolated using TRIZOL reagent (Ambion), and the RNA quality was checked on a 1% MOPS-Agarose gel. The samples were DNAse treated and cleaned and concentrated using the RNA clean and concentrator Kit (Zymo Research) and submitted to the UIUC Roy J Carver Sequencing core for library preparation and sequencing.

MOV10 eCLIP from N2A cells

Cell pellets from N2A cells were flash-frozen and sent to Eclipse BioInnovations. eCLIP was performed per (29) and as described in (6) except using the anti-MOV10 antibody (A301-571A; Bethyl Laboratories).

Phosphosite identification

Metal oxide affinity chromatography (SMOAC; Thermo Fisher Scientific) was used for phosphopeptide enrichment and separation of monophosphorylated and multiple phosphorylated species. The analysis was performed by directly injecting the enriched fractions onto an EASY-Spray (Cl8, 2 μm dp, 75 μm × 250 mm) column to avoid losing any phosphopeptides on a trapping column followed by gradient elution of the peptides sprayed directly into the model Orbitrap Lumos mass spectrometer using an EASY-Spray source. The instrument was operated in the HCD mode; however, if there was enough material, a second analysis using ETD fragmentation instead of HCD was performed. The MS and MS/MS data was processed using Proteome Discoverer 2.2 (Thermo Fisher Scientific) using the SEQUEST HT search engine with the phosphoRS node for site localization and validated with 1% FDR criteria using the Percolator algorithm.

MOV10 unfolding assay

MOV10 unfolding assay was performed as described (6).

AGO2 siRNA knockdown

0.5×10^6 N2A MOV10 KO cells were seeded in 6-well plate and after reaching 80% confluency, they were transfected with either AGO2 siRNA (ON-Target plus Mouse Ago2 siRNA, Cat #:L-058989-01-0005 (239528) siRNA, Dharmacon) or Irrelevant siRNA (Human PRMT9, Cat #: M-024046-00-0005, Dharmacon) using Lipofectamine 2000 (Thermo Fisher Scientific) and incubated overnight. Twenty four hours later, the cells were again transfected with siRNA and MOV10 S970D and incubated overnight. The next day, cells were lysed using TRIzol. As per manufacturer's protocol, the aqueous layer was used to isolate RNA for cDNA synthesis and qPCR. The organic layer was saved to extract protein sample for Western blotting to confirm AGO2 knockdown.

RNA isolation and RT-qPCR

RNA isolation, cDNA synthesis, and qRT-PCR was performed as described (6). The gene specific primers used are in Table S2.

Immunostaining of N2A cells

The staining protocol was performed as previously described (30) The primary antibodies used were as follows: rabbit MOV10 antibody (1:1000 dilution, Cat # A301-571A, Bethyl laboratories) and mouse-AGO2 antibody (1:300 dilution, Cat # ab57113, Abcam) or mouse-DDX6 antibody (1:300 dilution, SAB4200837, Sigma-Aldrich). The secondary antibodies used are as follows: Alexa fluor 594 donkey anti-rabbit (1:3000 dilution, Jackson ImmunoResearch, Cat # 711-585-152) and Alexa fluor 488 donkey anti-Mouse antibody, Jackson ImmunoResearch, Cat # 715-545-150). The samples were washed and mounted on slides with mounting media containing 4′,6-diamidino-2-phenylindole. Fluorescence images were obtained with DeltaVision OMX deconvolution microscope (GE Healthcare Life Sciences) using 100× 1.42 NA objective. A total of 86 and 67 0.2 μm thick z-stacks were acquired for AGO2 and DDX6 probed samples, respectively. The particles were counted using Analyze Particles plugin of ImageJ.

Data availability

All data are available in the main text or the supporting information and supporting tables. RNA-seq and eCLIP sequences are available at GEO GSE226241.

Supporting information—This article contains supporting information.

Acknowledgments—We thank Julija Sakutyte for preparing MOV10 plasmids. We also thank Dr Jenny Drnevich for the statistical analysis of the RNA-seq data and the Venn diagrams and Dr Erik Procko for helpful conversations about structure analysis. The findings and conclusions in this article are those of the authors and do not necessarily represent the views of the funding sources or the Centers for Disease Control and Prevention. This work was supported by Kiwanis Neuroscience Research Foundation, National Science Foundation NSF 1855474.

Author contributions—A. N., P. J. K., T. S., M. R., O. S., J. P., and S. C. investigation; A. N. and S. C. conceptualization; A. N. and S. C. writing–original draft; S. C. funding acquisition; S. C. supervision.

Conflict of interest—The authors declare that they have no conflicts of interest with the contents of this article.

Abbreviations—The abbreviations used are: AGO2, Argonaute 2; eCLIP, enhanced Cross-Linking Immunoprecipitation; MRE, miRNA recognition element; N2A, neuro 2a; RBP, RNA-binding protein; rG4s, G-quadruplex structure; S970, serine 970.

References

1. Friedman, R. C., Farh, K. K. H., Burge, C. B., and Bartel, D. P. (2009) Most mammalian mRNAs are conserved targets of microRNAs. *Genome Res.* **19**, 92–105
2. Meister, G., Landthaler, M., Peters, L., Chen, P. Y., Urlaub, H., Lührmann, R., *et al.* (2005) Identification of novel argonaute-associated proteins. *Curr. Biol.* **15**, 2149–2155
3. Gregersen, L. H., Schueler, M., Munschauer, M., Mastrobuoni, G., Chen, W., Kempa, S., *et al.* (2014) MOV10 is a 5′ to 3′ RNA helicase contributing to UPF1 mRNA target degradation by translocation along 3′ UTRs. *Mol. Cell* **54**, 573–585
4. Kenny, P. J., Zhou, H., Kim, M., Skariah, G., Khetani, R. S., Drnevich, J., *et al.* (2014) MOV10 and FMRP regulate AGO2 association with MicroRNA recognition elements. *Cell Rep.* **9**, 1729–1741
5. Kwok, C. K., Marsico, G., Sahakyan, A. B., Chambers, V. S., and Balasubramanian, S. (2016) rG4-seq reveals widespread formation of G-quadruplex structures in the human transcriptome. *Nat. Methods* **13**, 841–844
6. Kenny, P. J., Kim, M., Skariah, G., Nielsen, J., Lannom, M. C., and Ceman, S. (2020) The FMRP-MOV10 complex: a translational regulatory switch modulated by G-quadruplexes. *Nucleic Acids Res.* **48**, 862–878
7. Huang, H., Suslov, N. B., Li, N. S., Shelke, S. A., Evans, M. E., Koldobskaya, Y., *et al.* (2014) A G-quadruplex-containing RNA activates fluorescence in a GFP-like fluorophore. *Nat. Chem. Biol.* **10**, 686–691
8. Paige, J. S., Wu, K. Y., and Jaffrey, S. R. (2011) RNA mimics of green fluorescent protein. *Science* **333**, 642–646
9. Warner, K. D., Chen, M. C., Song, W., Strack, R. L., Thorn, A., Jaffrey, S. R., *et al.* (2014) Structural basis for activity of highly efficient RNA mimics of green fluorescent protein. *Nat. Struct. Mol. Biol.* **21**, 658–663
10. Banerjee, S., Neveu, P., and Kosik, K. S. (2009) A coordinated local translational control point at the synapse involving relief from silencing and MOV10 degradation. *Neuron* **64**, 871–884
11. Srinivasan, B., Samaddar, S., Mylavarapu, S. V. S., Clement, J. P., and Banerjee, S. (2021) Homeostatic scaling is driven by a translation-dependent degradation axis that recruits miRISC remodeling. *PLoS Biol.* **19**, e3001432
12. Golden, R. J., Chen, B., Li, T., Braun, J., Manjunath, H., Chen, X., *et al.* (2017) An argonaute phosphorylation cycle promotes microRNA-mediated silencing. *Nature* **542**, 197–202
13. Wang, X., Han, Y., Dang, Y., Fu, W., Zhou, T., Ptak, R. G., *et al.* (2010) Moloney leukemia virus 10 (MOV10) protein inhibits retrovirus replication. *J. Biol. Chem.* **285**, 14346–14355
14. Olsen, J. V., Vermeulen, M., Santamaria, A., Kumar, C., Miller, M. L., Jensen, L. J., *et al.* (2010) Quantitative phosphoproteomics revealswide-spread full phosphorylation site occupancy during mitosis. *Sci. Signal.* **3**, ra3
15. Skariah, G., Seimetz, J., Norsworthy, M., Lannom, M. C., Kenny, P. J., Elrakhawy, M., *et al.* (2017) Mov10 suppresses retroelements and regulates neuronal development and function in the developing brain. *BMC Biol.* **15**, 54
16. Moore, M. J., Scheel, T. K. H., Luna, J. M., Park, C. Y., Fak, J. J., Nishiuchi, E., *et al.* (2015) MiRNA-target chimeras reveal miRNA 3′-end pairing as a major determinant of argonaute target specificity. *Nat. Commun.* **6**, 1–17
17. Liu, C., Zhang, X., Huang, F., Yang, B., Li, J., Liu, B., *et al.* (2012) APOBEC3G inhibits microRNA-mediated repression of translation by interfering with the interaction between Argonaute-2 and MOV10. *J. Biol. Chem.* **287**, 29373–29383
18. Ayache, J., Bénard, M., Ernoult-Lange, M., Minshall, N., Standart, N., Kress, M., *et al.* (2015) P-body assembly requires DDX6 repression complexes rather than decay or Ataxin2/2L complexes. *Mol. Biol. Cell* **26**, 2579–2595
19. Hubstenberger, A., Courel, M., Mozziconacci, J., Kress, M., and Weil, D. (2017) P-body purification reveals the condensation of repressed mRNA regulons. *Mol. Cell* **68**, 144–157.e5
20. Jumper, J., Evans, R., Pritzel, A., Green, T., Figurnov, M., Ronneberger, O., *et al.* (2021) Highly accurate protein structure prediction with AlphaFold. *Nature* **596**, 7873
21. Piovesan, D., Necci, M., Escobedo, N., Monzon, A. M., Hatos, A., Mičetić, I., *et al.* (2021) MobiDB: intrinsically disordered proteins in 2021. *Nucleic Acids Res.* **49**, D361–D367
22. Kato, M., Han, T. W., Xie, S., Shi, K., Du, X., Wu, L. C., *et al.* (2012) Cell-free formation of RNA granules: low complexity sequence domains form dynamic fibers within hydrogels. *Cell* **149**, 753–767
23. Siomi, M. C., Zhang, Y., Siomi, H., and Dreyfuss, G. (1996) Specific sequences in the fragile X syndrome protein FMR1 and the FXR proteins mediate their binding to 60S ribosomal subunits and the interactions among them. *Mol. Cell. Biol.* **16**, 3825–3832
24. Chen, E., Sharma, M. R., Shi, X., Agrawal, R. K., and Joseph, S. (2014) Fragile X mental retardation protein regulates translation by binding directly to the ribosome. *Mol. Cell* **54**, 407–417
25. Abdelmohsen, K., Tominaga, K., Lee, E. K., Srikantan, S., Kang, M. J., Kim, M. M., *et al.* (2011) Enhanced translation by nucleolin via G-rich elements in coding and non-coding regions of target mRNAs. *Nucleic Acids Res.* **39**, 8513–8530
26. Luo, E. C., Nathanson, J. L., Tan, F. E., Schwartz, J. L., Schmok, J. C., Shankar, A., *et al.* (2020) Large-scale tethered function assays identify factors that regulate mRNA stability and translation. *Nat. Struct. Mol. Biol.* **27**, 989–1000
27. Buchser, W. J., Slepak, T. I., Gutierrez-Arenas, O., Bixby, J. L., and Lemmon, V. P. (2010) Kinase/phosphatase overexpression reveals pathways regulating hippocampal neuron morphology. *Mol. Syst. Biol.* **6**, 391
28. Furtak, V., Mulky, A., Rawlings, S. A., Kozhaya, L., Lee, K. E., KewalRamani, V. N., *et al.* (2010) Perturbation of the P-body component Mov10 inhibits HIV-1 infectivity. *PLoS One* **5**, e9081
29. van Nostrand, E. L., Pratt, G. A., Shishkin, A. A., Gelboin-Burkhart, C., Fang, M. Y., Sundararaman, B., *et al.* (2016) Robust transcriptome-wide discovery of RNA-binding protein binding sites with enhanced CLIP (eCLIP). *Nat. Methods* **13**, 508–514
30. Lannom, M. C., Nielsen, J., Nawaz, A., Shilikbay, T., and Ceman, S. (2021) FMRP and MOV10 regulate Dicer1 expression and dendrite development. *PLoS One* **16**, e0260005
31. Fairman-Williams, M. E., Guenther, U. P., and Jankowsky, E. (2010) SF1 and SF2 helicases: family matters. *Curr. Opin. Struct. Biol.* **20**, 313–324
32. Nawaz, A., Shilikbay, T., Skariah, G., and Ceman, S. (2022) Unwinding the roles of RNA helicase MOV10. *Wiley Interdiscip. Rev. RNA* **13**, e1682